ELSEVIER

Biophysical Chemistry 113 (2005) 53–59

Biophysical Chemistry

www.elsevier.com/locate/bpc

Binding of 5,10,15,20-tetrakis(*N*-methylpyridinium-4-yl)-21*H*,23*H*-porphyrin to an AT-Rich Region of a Duplex DNA

Takako Ohyama, Hajime Mita, Yasuhiko Yamamoto*

Department of Chemistry, University of Tsukuba, 1-1-1 Ten-O-Dai, Tsukuba 305-8571, Japan

Received 25 June 2004; received in revised form 24 July 2004; accepted 26 July 2004
Available online 2 October 2004

Abstract

Characterization of the interaction between DNA and small organic compounds is of considerable importance for gaining insights into the mechanism underlying molecular recognition, which could be highly relevant to drug design. In the present study, the interaction of a water-soluble cationic porphyrin, 5,10,15,20-tetrakis(*N*-methylpyridinium-4-yl)-21*H*,23*H*-porphyrin, with a self-complementary duplex DNA, $d(GCTTAAGC)_2$, has been investigated by means of absorption, circular dichroism, and NMR spectroscopies. The optical studies indicated that TMPyP binds to the TTAA region of $d(GCTTAAGC)_2$ with a binding constant of 2.5×10^6 M^{-1} and a stoichiometric ratio of 1:1. The observation of intermolecular nuclear Overhauser effect connectivities demonstrated that TMPyP binds in the major groove of $d(GCTTAAGC)_2$. A model for the binding of TMPyP in the major groove of the AT-rich region of $d(GCTTAAGC)_2$ is proposed.

Keywords: DNA-interactive compound; Molecular recognition; NMR; Nuclear Overhauser effect; Porphyrin derivative; Self-complementary duplex DNA

1. Introduction

5,10,15,20-Tetrakis(*N*-methylpyridinium-4-yl)-21*H*,23*H*-porphyrin (TMPyP; Fig. 1) is a water-soluble cationic porphyrin and has been the subject of extensive study, especially in relation to its unique physicochemical properties leading to interaction with nucleic acids, as well as its therapeutic application [1]. TMPyP comprises a porphyrin core and *N*-methylpyridinium side chains. The planarity and hydrophobicity of the porphyrin ring are well suited for intercalation into the base pairs of nucleic acids. Furthermore, the porphyrin ring is responsible for the production of singlet oxygen [2], which can be used to damage DNA in tumor cells when it is used as a photosensitizing agent in photodynamic therapy [3–5]. On the other hand, the relatively high water solubility of TMPyP is largely attributable to the charged peripheral side chains which prevent self-aggregation. Additionally, the positively charged side chains of TMPyP are suited for electrostatic interaction with nucleic acids, which are negatively charged polyelectrolytes.

TMPyP has been shown to bind to various forms of nucleic acids such as duplex DNA [6–11] and RNA [12], a DNA–RNA hybrid [12], triplex DNA [13,14], and quadruplex DNA [15–19]. The mode of binding of TMPyP to duplex DNA has been shown to depend greatly on the DNA sequence and the solution conditions. TMPyP has been shown to intercalate into GC-rich regions, and the molecular recognition upon the intercalation of TMPyP into GC-rich sequences has been characterized in detail through solution NMR studies on the complexes [9,20,21]. On the other hand, DNA footprinting [6], linear dichroism [10], and fluorescence [7] studies on the interaction of TMPyP with AT-rich sequences of duplex DNA have shown that TMPyP favors surface binding, with binding constants comparable to those for intercalation, at low TMPyP to DNA base ratios and, as the ratio increases, TMPyP has been shown to form a moderate or extensive stacking array along the DNA strand [9,20–24]. Thus, in contrast to the detailed knowledge, at the atomic level, on the interaction of TMPyP with GC-rich sequences, the nature of the molecular recognition

* Corresponding author. Tel.: +81 29 853 6521; fax: +81 29 853 6521.
E-mail address: yamamoto@chem.tsukuba.ac.jp (Y. Yamamoto).

0301-4622/$ - see front matter © 2004 Elsevier B.V. All rights reserved.
doi:10.1016/j.bpc.2004.07.039

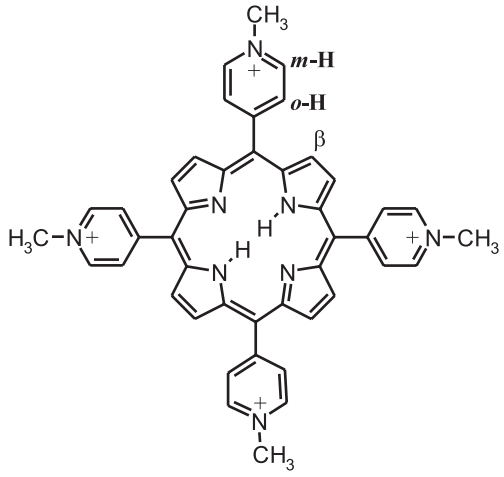

Fig. 1. Molecular structure of 5,10,15,20-tetrakis(*N*-methyl-pyridinium-4-yl)-21*H*,23*H*-porphyrin (TMPyP).

between TMPyP and AT-rich sequences has remained in depth to be explore.

Various aromatic compounds have been shown to bind preferentially in the minor groove of the AT-rich region of duplex DNA [25, 26]. In general, minor groove binders adopt curved shapes that fit the turn of duplex DNA in the minor groove. When the AT sequences are replaced by GC ones, the minor groove binders tend to exhibit intercalative binding. Since the amine groups of guanine bases in GC sequences stick out into the minor groove, the steric repulsion between an aromatic compound and the amine groups of guanine bases in the minor groove has been thought to play a major role in determining the mode of binding of DNA-interactive compounds.

TMPyP shares structural features with conventional minor groove binders [10,11], and hence minor groove binding might be expected for the interaction of TMPyP with the AT-rich region of duplex DNA. But, as has been shown for the influence of the DNA sequence on the binding mode propensity of DNA-interactive compounds [27–31], elucidation of the interaction of TMPyP with the AT-rich region is necessary for a detailed understanding of the molecular recognition upon the binding of TMPyP to DNA, which could provide useful information for designing photosensitizing agents possessing even greater DNA binding specificity. In the present study, the interaction of TMPyP with a self-complementary oligonucleotide, $d(GCTTAAGC)_2$, was characterized by means of optical absorption (Vis), circular dichroism (CD), and NMR spectroscopies to gain insights into the molecular recognition on the binding of TMPyP to the AT sequences of duplex DNA. The Scatchard plots of the Soret absorbance of TMPyP obtained upon titration with $d(GCTTAAGC)_2$ were found to be straight lines, and revealed the binding constant of 2.5×10^6 M^{-1}, and a stoichiometric ratio of 1:1 between TMPyP and $d(GCTTAAGC)_2$. An induced positive CD band in the Soret region, observed for a solution mixture of TMPyP and $d(GCTTAAGC)_2$, strongly suggested groove binding of TMPyP to $d(GCTTAAGC)_2$. Additionally, the observation of intermolecular nuclear Overhauser effect (NOE) connectivities demonstrated that TMPyP in the complex is located in the major groove of $d(GCTTAAGC)_2$. Finally, a molecular model that accounts for the binding of TMPyP in the major groove of the AT-rich region of duplex DNA is proposed.

2. Experimental

2.1. Sample preparation

$d(GCTTAAGC)_2$ purified with a C-18 Sep-Pak cartridge was purchased from Espec Oligo Service (Tsukuba, Japan). The oligonucleotide was collected by ethanol precipitation, and then desalted with Microcon YM-3 (Millipore, Bedford, MA). The concentration of the oligonucleotide was determined spectrophotometrically using the absorption value at 260 nm ($\varepsilon_{260}=8.76\times10^7$ cm M^{-1}). TMPyP tosylate was purchased from Dojin Kagaku (Kumamoto, Japan), and was converted to the chloride salt as follows. TMPyP tosylate was dissolved in distilled water and then a KI solution was added to the TMPyP solution to precipitate the iodide salt of TMPyP. The precipitated iodide salt of TMPyP was dissolved in 0.1 N HCl and then applied to an ion-exchange column (Dowex 1×2 Cl^- form resin, mesh size 200–400 nm, Dow Chemicals, Midland, MI) to replace the counter anion with the chloride ion. The TMPyP concentration was determined using the extinction coefficient of $\varepsilon_{424}=2.26\times10^6$ cm M^{-1}. Sodium phosphate buffer (100 mM, pH 7.0, containing 50 mM NaCl) was used as the solvent throughout the optical measurements. For NMR measurements, the oligonucleotide duplex concentration was 2 mM, as a duplex form, in 50 mM NaCl and 100 mM sodium phosphate buffer, pH 7.0; The ^2H_2O content in the samples was either ~10% or ~100%.

2.2. Absorption and CD spectroscopies

Absorption spectra were recorded on a Beckman DU640 spectrometer over the spectral range of 200–600 nm. CD spectra were recorded on a JASCO J-720W spectrometer over the spectral range of 240–500 nm. The concentrations of TMPyP for the absorption and CD measurements were 3.0 and 6.0 μM, respectively. The melting temperatures (T_m) of 4.5 μM $d(GCTTAAGC)_2$ in the absence and presence of a stoichiometric amount of TMPyP were determined from the temperature dependence of the hyperchromic effect on the absorbance at 260 nm. The temperature for each measurement was increased over the temperature range of 15–90 °C, with a heating rate of 0.5 °C min^{-1}.

2.3. NMR measurement

^1H NMR spectra were recorded on a Bruker AVANCE-500 or 600 spectrometer operating at a ^1H frequency of 500 or 600 MHz, respectively. 1D ^1H NMR spectra were obtained

with a 25 ppm spectral width, 32 k data points, a 2 s relaxation delay, and 64 transients. Water suppression was achieved with the watergate method [32,33]. The signal-to-noise ratio of the spectrum was improved by apodization, which introduced 1-Hz line broadening. NOESY spectra were acquired by quadrature detection in the phase-sensitive mode with a States-TPPI [34] with a 12,500-Hz spectral width, 2048×512 data points, a 2-s relaxation delay, and a mixing time of 60, 120, or 300 ms. A phase-shifted sine-squared window function was applied to both dimensions before 2D Fourier transformation. Chemical shifts are referred to external 2,2-dimethyl-2-silapentane-5-sulfonate (DSS).

3. Results

3.1. Absorption and CD spectra

We first studied the interaction between TMPyP and d(GCTTAAGC)$_2$ on the basis of the absorption and CD spectral changes of the porphyrin π-system of TMPyP. The absorption and CD spectra of TMPyP in the presence of various concentrations of d(GCTTAAGC)$_2$ are shown in A and B of Fig. 2, respectively. As shown in Fig. 2A, the Soret band of TMPyP red-shifted from 422 to 431 nm on the addition of d(GCTTAAGC)$_2$ and exhibited about 14% hypochromicity. These results clearly indicated that the porphyrin π-system of TMPyP interacts with d(GCTTAAGC)$_2$. In addition, the observation of a clear isosbestic point at 425.5 nm over the range of 1.5–5.0 for R (=[TMPyP]/[d(GCTTAAGC)$_2$]) demonstrated that a specific interaction occurs between TMPyP and d(GCTTAAGC)$_2$. Furthermore, the addition of d(GCTTAAGC)$_2$ to TMPyP induced a positive CD band in the Soret region, as shown in Fig. 2B.

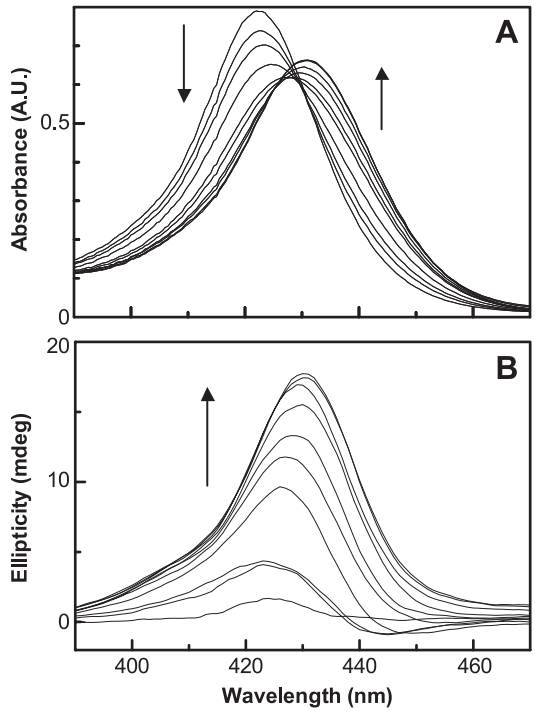

Fig. 2. Vis absorption (A) and CD (B) spectra, 390–470 nm, of TMPyP in the presence of various concentrations of d(GCTTAAGC)$_2$ at 25 °C. [TMPyP]=3.0 and 6.0 μM for the absorption and CD measurements, respectively. R([TMPyP]/[d(GCTTAAGC)$_2$]) was varied from 0 to 5.0. Isosbestic point was observed at 425.5 nm in panel (A).

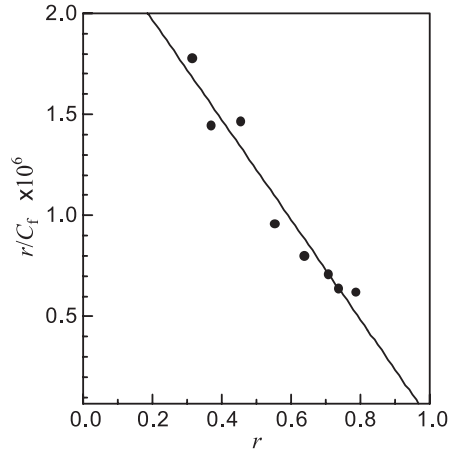

Fig. 3. Scatchard plots of the Soret absorbance at 440 nm. Slope of the fitted line was -2.5×10^6, the y- and x-intercepts were 2.5×10^6 and 0.99, respectively, with a square multiple correlation coefficient r^2=0.948. The plots revealed a binding constant of 2.5×10^6 M^{-1} and a stoichiometric ratio of about 1:1 between TMPyP and the oligonucleotide.

A Scatchard plot of the absorption at 440 nm is shown in Fig. 3. The binding ratio r is defined as C_b/[d(GCTTAAGC)$_2$], where C_b is obtained from 440 nm absorbance change (ΔA) exerted by addition of d(GCTTAAGC)$_2$, and molar extinction coefficients at 440 nm determined for solutions with R=0 and 10.0 ($\varepsilon_{R=0}$ and $\varepsilon_{R=10.0}$, respectively), through the equation, $C_b=\Delta A/(\varepsilon_{R=0}-\varepsilon_{R=10.0})$. This plot could be satisfactorily represented as a straight line, yielding a value of 2.5×10^6 M^{-1} for the binding constant for TMPyP and d(GCTTAAGC)$_2$, with a stoichiometric ratio of 1:1.

3.2. Melting temperature of d(GCTTAAGC)$_2$

The interaction of d(GCTTAAGC)$_2$ with TMPyP was also reflected by an increased melting temperature (T_m) of duplex DNA. On analysis of the temperature dependence of the absorption at 260 nm, the T_m value of 26 °C was obtained for 4.5 μM d(GCTTAAGC)$_2$ and this value increased by ~14 °C in the presence of a stoichiometric amount of TMPyP relative to d(GCTTAAGC)$_2$. This result demonstrated that d(GCTTAAGC)$_2$ was significantly stabilized on the binding of TMPyP.

3.3. NMR spectroscopy

A 600-MHz ^{1}H NMR spectrum of d(GCTTAAGC)$_2$ at 25 °C is illustrated in Fig. 4A. Since the concentration of d(GCTTAAGC)$_2$ used for the NMR measurement was greater by a factor of 40, its T_m value should be much higher

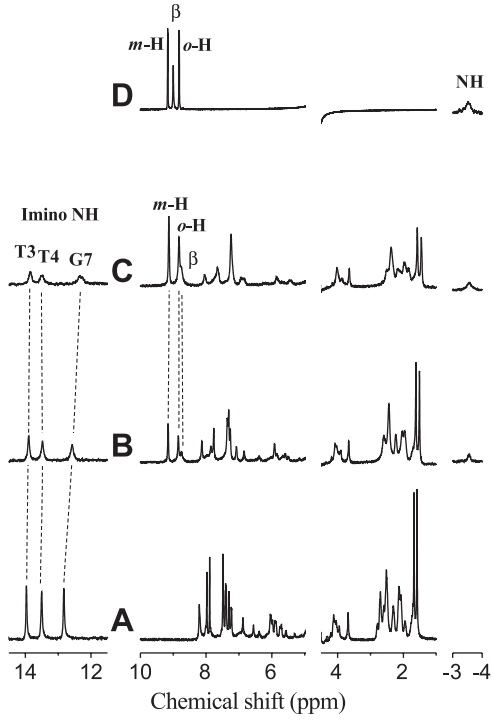

Fig. 4. The 600 MHz ^{1}H NMR spectra of d(GCTTAAGC)$_2$ (A), solution mixtures with R([TMPyP]/[d(GCTTAAGC)$_2$])=0.5 (B) and 1.0 (C), and TMPyP (D) in 100 mM sodium phosphate buffer, pH 7.0, with 50 mM NaCl at 25 °C. Most DNA signals were shifted upfield and broadened with increasing R values.

than that determined spectrophotometrically. Signal assignments were made, using standard 2D NMR methods (not shown), and are listed in Table 1. The imino proton signals due to T3, T4, and G7 were resolved in the downfield-shifted region. The G1 imino proton signal was not visible in the spectrum and could be underneath the G7 imino proton signal. The chemical shifts of the signals of d(GCTTAAGC)$_2$ were affected by the addition of TMPyP (traces B and C in Fig. 4). Upon the addition of TMPyP, most signals of d(GCTTAAGC)$_2$ exhibited progressive shifts. This demonstrated not only that the electronic structure of d(GCTTAAGC)$_2$ is affected by the interaction with TMPyP, but also that the time scale of the complex formation between them is faster compared with the NMR time scale. The TMPyP-induced shift changes of the DNA signals are summarized in Table 1. The DNA signals exhibited sizable upfield shifts upon the addition of TMPyP. Considering the small size of d(GCTTAAGC)$_2$, it was not surprising that most of the DNA signals were affected by the binding of TMPyP.

The shifts and line widths of the signals of TMPyP were also affected by the interaction with d(GCTTAAGC)$_2$. The β-pyrrole, and *o*- and *m*-proton signals of TMPyP exhibited upfield shifts upon the addition of d(GCTTAAGC)$_2$, whereas the shift of the pyrrole NH proton signal of TMPyP was essentially unaffected by the addition of d(GCTTAAGC)$_2$. Further addition of TMPyP to d(GCTTAAGC)$_2$ resulted in considerable broadening and/or DNA signals (spectra not shown), indicating either a dramatic increase in

Table 1
^{1}H NMR shifts (ppm) of d(GCTTAAGC)$_2$ and shift change $\Delta\delta^a$ (ppm) induced upon the addition of a half stoichiometric amount of TMPyP in 100 mM sodium phosphate buffer, pH 7.0, and 50 mM NaCl at 25 °C

	H1′		H2′		H2″		H3′		H4′		H6/H8		H2/H5/Me		amino		imino		TMPyP		
	free	Dd	free	Dd	free	Dd	free	Dd	free	Dd	free	Dd	free	Dd	free	Dd	free	Dd		free	Dd
G1	5.95	−0.29	2.64	−0.19	2.76	−0.17	4.84	n.d.	n.a.	n.d.	7.94	−0.19	–	–	8.09	−0.13	–	–	*m*-H	9.21	−0.08
C2	6.10	−0.20	2.21	−0.17	2.56	−0.33	4.84	n.d.	4.27	n.d.	7.53	−0.19	5.33	−0.20	8.24	n.d.	–	–	*o*-H	8.82	0.00
T3	6.04	−0.13	2.14	−0.12	2.56	−0.13	4.87	−0.11	4.18	n.d.	7.45	−0.14	1.64	−0.14	–	–	14.06	−0.19	b	9.00	−0.30
T4	5.63	−0.14	2.01	−0.09	2.35	−0.12	4.87	−0.11	4.10	n.d.	7.37	−0.11	1.73	−0.13	–	–	13.60	−0.15	NH	−3.60	0.00
A5	5.80	−0.18	2.75	−0.14	2.86	−0.12	5.04	−0.15	4.39	n.d.	8.28	−0.14	6.92	−0.10	–	–	–	–			
A6	5.93	−0.21	2.58	n.d.	2.77	n.d.	5.01	n.d.	4.40	n.d.	8.04	−0.17	7.45	−0.17	–	–	–	–			
G7	5.76	−0.18	2.37	−0.16	2.59	−0.17	4.90	−0.14	4.31	n.d.	7.54	−0.19	–	–	6.63	n.d.	12.89	−0.32			
C8	6.06	−0.25	2.16	n.d.	2.20	n.d.	n.a.	n.d.	4.00	n.d.	7.24	−0.20	5.05	−0.29	6.43	n.d.	–	–			

n.a. Not assigned.
n.d. Not determined due to the lack of the signal assignments for both systems.
[a] $\Delta\delta=\delta_{R=0.5}-\delta_{R=0}$, where $R=\frac{[\text{TMPyP}]}{[\text{d(GCTTAAGC)}_2]}$.

the apparent molecular weight of d(GCTTAAGC)$_2$ and/or structural inhomogeneity of the complex in the presence of a large excess of TMPyP. Therefore, in the presence of excess TMPyP, the binding of TMPyP to d(GCTTAAGC)$_2$ is likely to be non-specific.

The observation of intermolecular NOEs between TMPyP and d(GCTTAAGC)$_2$ could provide direct information regarding the structure of the TMPyP–DNA complex. Portions of the NOESY spectra for the solution mixture of d(GCTTAAGC)$_2$ and TMPyP with R=0.5, recorded with a series of mixing times, are illustrated in Fig. 5. With a short mixing time (60 ms), the *o*- and *m*-protons of TMPyP exhibited rather specific intermolecular NOE connectivities to the T3 H1′, A6 H1′ and A5 H1′, A6 H1′ protons of d(GCTTAAGC)$_2$, respectively. In addition, both the β-pyrrole and *o*-protons of TMPyP exhibited weak intermolecular NOE connectivity to the T3 2′ proton of d(GCTTAAGC)$_2$. With increasing mixing times, the H1′ protons of T3, T4, A5, and A6 of d(GCTTAAGC)$_2$ exhibited NOE connectivities with the *o*- and *m*-protons of TMPyP. Furthermore, most of the DNA protons exhibiting NOE connectivities with TMPyP protons are located in the major groove of duplex DNA, so TMPyP is likely to be accommodated in the major groove.

The conformation of d(GCTTAAGC)$_2$ complexed with TMPyP may be inferred from the intramolecular NOE connectivities. The intraresidue NOE connectivities between

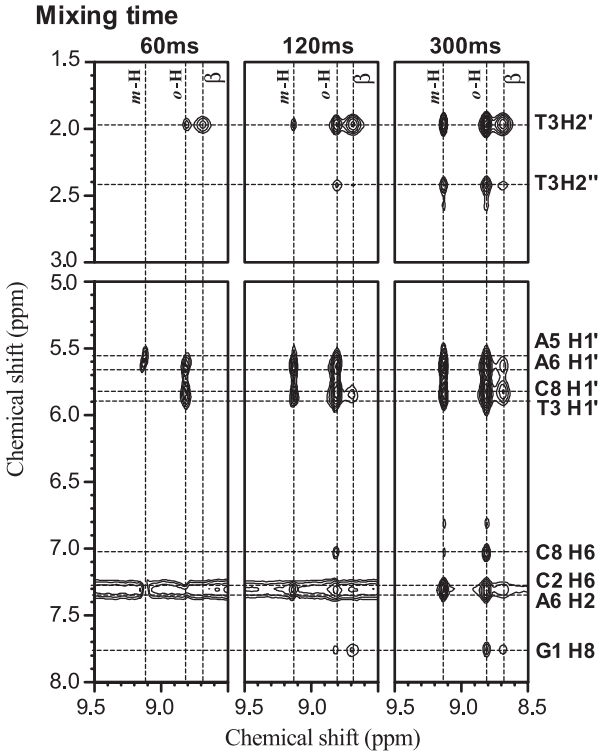

Fig. 5. Portions of NOESY spectra of a solution mixture with an R value of 0.5 at 25 °C, recorded using a series of mixing times: 60, 120 and 300 ms. Build-up of the cross peaks between TMPyP aromatic ring protons and T3 (H1′/H2′/H6), G7 H1′ (strong), and C2 (H2″/H6) G7 H8 (weak) was observed.

the base and deoxyribose protons of duplex DNA have provided a convenient signature for its conformation in solution. The observation of NOE connectivities between the H6 and H2′/H2″ protons for A and T residues, and between the H8 and H2′/H2″ protons for C and G residues clearly indicated that d(GCTTAAGC)$_2$ in the complex with TMPyP adopts a typical B-type duplex, and hence the binding of TMPyP does not significantly affect the conformation of d(GCTTAAGC)$_2$. Furthermore, ^{31}P NMR signals for d(GCTTAAGC)$_2$ in the presence of various concentrations of TMPyP were observed in the chemical shift region expected for a typical B-type duplex (results not shown). These results strongly suggested that the conformation of d(GCTTAAGC)$_2$ is independent of TMPyP binding.

4. Discussion

4.1. Binding of TMPyP to d(GCTTAAGC)$_2$

The red shift and hypochromicity of the Soret absorption band, as well as the induced positive CD band of TMPyP in the presence of d(GCTTAAGC)$_2$ (Fig. 2A and B), demonstrated that the porphyrin π-system of TMPyP interacts with d(GCTTAAGC)$_2$. It has been reported that intercalation of TMPyP into for CG pairs of duplex DNA induced a red shift of Soret absorption from 422 nm to 440 nm, together with high hypochromicity (~50%) of the band; there was an induced negative CD band in the Soret region as well [20]. However, in the case of surface binding of TMPyP to the AT base pairs of duplex DNA, the Soret absorption exhibited a red shift from 422 to 430 nm, and relatively low hypochromicity (~20%), along with an induced positive CD band in the Soret region [20]. Therefore, the observed changes in both the absorption and CD spectra of TMPyP, induced by the addition of d(GCTTAAGC)$_2$, were consistent with the surface binding of TMPyP to the AT base pairs of d(GCTTAAGC)$_2$, and the absence of direct interaction between the porphyrin π-system of TMPyP and the base pairs of d(GCTTAAGC)$_2$. d(GCTTAAGC)$_2$ possesses four AT pairs at the center of its strand. According to the conformation of a typical B-form of duplex DNA, four consecutive base pairs span about 10 nm, which is almost the same as the diameter of TMPyP. Therefore, TMPyP is expected to bind to the center TTAA of d(GCTTAAGC)$_2$.

The affinity of TMPyP to d(GCTTAAGC)$_2$ could be determined by Scatchard plot analysis of the Soret absorbance (Fig. 3). The plot demonstrated 1:1 complex formation between TMPyP and d(GCTTAAGC)$_2$, and a binding constant of 2.5×10^6 M^{-1}. The obtained binding constant was within the range of values, i.e., 10^4–10^{10} M^{-1}, reported for various DNA-interactive compounds [27–31]. Various interactions are expected to contribute to stabilization of the TMPyP–DNA complex. An electrostatic interaction between the *N*-methylpyridinium of TMPyP and the phosphodiester backbone of d(GCTTAAGC)$_2$ could potentially regulate both

the molecular recognition between the two and the stability of the complex. Yet in the presence of a relatively high salt concentration in the system, the contribution of the electrostatic interaction to the relatively high affinity of TMPyP to d(GCTTAAGC)$_2$ might be rather small.

4.2. Structure of the TMPyP–DNA complex

The structure of the TMPyP–DNA complex in solution could be inferred on analysis of the intermolecular NOE connectivities between them. With short mixing times, specific intermolecular NOE connectivities of the *o*- and *m*-protons of TMPyP to the T3 H1′, A6 H1′ and A5 H1′, A6 H1′ protons of d(GCTTAAGC)$_2$, respectively, were observed, and these connectivities strongly suggested that the *N*-methylpyridinium side chains of TMPyP are accommodated in the major groove of d(GCTTAAGC)$_2$ in the complex. A molecular model for the structure of TMPyP–DNA complex could thus be inferred (see below).

Most ^{1}H NMR signals for d(GCTTAAGC)$_2$ exhibited progressive chemical shift changes upon binding TMPyP. This demonstrated the fast exchange between bound and free DNA, which is consistent with the groove binding of TMPyP to d(GCTTAAGC)$_2$. Most signals for d(GCTTAAGC)$_2$ were affected by the binding of TMPyP, and relatively large TMPyP-induced shifts were observed even for the signals due to the terminal GC residues of d(GCTTAAGC)$_2$. Molecular modeling showed that the *N*-methylpyridinium side chains of TMPyP are located in the proximity of the terminal GC residues in the TMPyP-d(GCTTAAGC)$_2$ complex (see below). Therefore, the relatively large chemical shift perturbations of the signals of the terminal GC residues in the complex would be due to the influence of the nearby *N*-methylpyridinium side chains of TMPyP.

Although the orientation of TMPyP with respect to the major groove of d(GCTTAAGC)$_2$ in the complex could not be determined quantitatively on analysis of these results, a molecular modeling docking study was performed to explain the structural features of the complex as well as the molecular recognition upon the complex formation. Assuming that TMPyP binds across both strands of the duplex DNA to account for the greatly elevated T_m value for the complex, relative to that for d(GCTTAAGC)$_2$, and that the conformation of d(GCTTAAGC)$_2$ in the complex remains a typical B-type duplex, as reflected by the intraresidue NOESY connectivities and ^{31}P NMR shifts, a qualitative model was obtained for TMPyP-d(GCTTAAGC)$_2$ complex, as illustrated in Fig. 6. The model was not generated with an energy minimization algorithm, but was constructed on the basis of simple docking between the two molecules to satisfy the observed intermolecular NOE connectivities. In the model, TMPyP fitted well in the major groove of the self-complementary duplex DNA, and the symmetric nature of the molecular structure of the complex was preserved as much as possible. We suppose that the preservation of the molecular symmetry of the complex contributes to its high thermodynamic stability. Four different modes of docking of C_4 symmetric TMPyP to the duplex DNA are identical in thermodynamic stability and dynamic interconversion between them is expected in solution. In addition to the structure of the TMPyP–DNA complex schematically illustrated in Fig. 6, alternative orientations of TMPyP within the major groove of the DNA might be possible. But not only intermolecular contacts, but also molecular symmetry of the complex in other docking models should be considerably reduced compared with those in the model of Fig. 6.

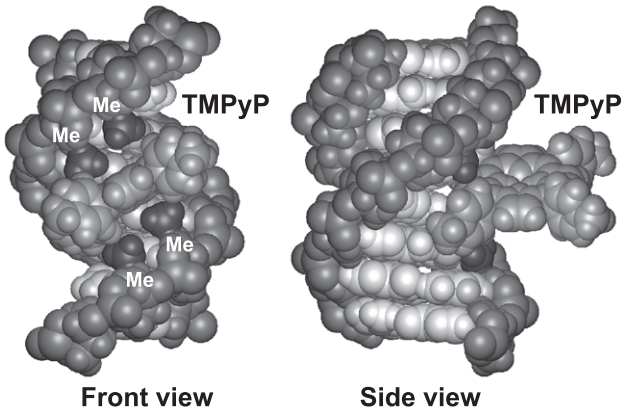

Fig. 6. Schematic representation of a model for the TMPyP-d(GCTTAAGC)$_2$ complex. The phosphodiester backbone of the duplex DNA is shown in dark gray, and the methyl groups of T3 and T4 are represented in darker gray and denoted by Me. TMPyP binds in the major groove of the central TTAA sequence of the oligonucleotide. Since the methyl groups of T3 and T4 of the oligonucleotide stick out into the major groove, the major groove of the TTAA region becomes narrower and hence provides a suitable pocket for TMPyP binding. The symmetry of the molecular structure was preserved as much as possible to construct the model.

The size of the groove in duplex DNA depends upon the sequence, and so the major groove of the AT-rich region becomes less deep, as shown in Fig. 6. Since the methyl groups of T3 and T4 of d(GCTTAAGC)$_2$ protrude into the major groove of this oligonucleotide, as indicated in Fig. 6, the major groove of the TTAA region becomes narrower and hence is expected to provide a more suitable pocket for TMPyP binding than the minor groove. This steric interaction is probably significant for the molecular recognition between TMPyP and duplex DNA. Furthermore, the structural features of the complex, as highlighted in the qualitative model in Fig. 6, demonstrated that hydrophobic and van der Waals interactions, together with an electrostatic interaction, contribute significantly to stabilization of the complex. The positively charged peripheral side chains and π-systems of TMPyP facilitate attraction to the DNA molecule through non-specific electrostatic and hydrophobic interactions, respectively. Since the orientation of TMPyP with respect to DNA in the complex was determined thermodynamically to give the minimum energy of the system, the van der Waals interaction between TMPyP and d(GCTTAAGC)$_2$ possibly plays a significant role in the specific binding of TMPyP to DNA. Thus, the major groove-binding propensity of TMPyP

as to duplex DNA is regulated by structural features of the groove provided by the sequence.

Acknowledgements

The authors wish to thank Professor David H. Peyton (Portland State University) for the helpful discussions. This work was partly supported by a Grant-in-Aid (No. 15550143) from the Ministry of Education, Science, and Culture of Japan.

References

[1] R.J. Fiel, Porphyrin–nucleic acid interactions: a review, J. Biomol. Struct. Dyn. 6 (1989) 1259–1274.
[2] J.B. Verlhac, A. Gaudemer, Water-soluble porphyrins and metalloporphyrins as photosensitizers in aerated aqueous solutions: I. Detection and determination of quantum yield of formation of singlet oxygen, Nouv. J. Chim. 8 (1984) 401–406.
[3] A. Villanueava, A. Juarranz, V. Diaz, J. Gomez, M. Canete, Photodynamic effects of a cationic mesosubstituted porphyrin in cell culture, Anti-cancer Drug Des. 7 (1992) 297–303.
[4] E. Izbicka, D. Nishioka, V. Marcell, E. Raymond, K.K. Davidson, R.A. Lawrence, R.T. Wheelhouse, L.H. Hurley, R.S. Wu, D.D. Von Hoff, Telomere-interactive agents affect proliferation rates and induce chromosomal destabilization in sea urchin embryos, Anti-Cancer Drug Des. 14 (1999) 355–365.
[5] S.Y. Rha, E. Izbicka, R. Lawrence, K. Davidson, D. Sun, M.P. Moyer, G.D. Roodman, L.H. Hurley, D.D. Von Hoff, Effect of telomere and telomerase interactive agents on human tumor and normal cell lines, Clin. Cancer Res. 6 (2000) 987–993.
[6] K.G. Ford, S. Neidle, Perturbation in DNA structure upon interaction with porphyrin revealed by chemical probes, DNA footprinting and molecular modeling, Bioorg. Med. Chem. 3 (1995) 671–677.
[7] S.C.M. Gandini, L.E. Borissevitch, J.R. Perussi, H. Imasato, M. Tabak, Aggregation of *meso*-tetrakis(4-*N*-methyl-pyridiniumyl) porphyrin in its free base, Fe(III) and Mn(III) forms due to the interaction with DNA in aqueous solutions: optical absorption, fluorescence and light scattering studies, J. Lumin. 78 (1998) 53–61.
[8] R.T. Wheelhouse, D. Sun, H. Han, F.X. Han, L.H. Hurley, Cationic porphyrins as telomerase inhibitors: the interaction of tetra-(*N*-methyl-4-pyridyl)porphine with quadruplex DNA, J. Am. Chem. Soc. 120 (1998) 3261–3262.
[9] A.B. Guliaev, N.B. Leontis, Cationic 5,10,15,20-tetrakis(*N*-methylpyridinium- 4-yl)porphyrin fully intercalates at 5′-CG-3′ step of duplex DNA solution, Biochemistry 38 (1999) 15425–15437.
[10] S. Lee, Y.A. Lee, H.M. Lee, J.Y. Lee, D.H. Kim, S.K. Kim, Rotation of periphery methylpyridine of *meso*-tetrakis(*N*-methypyridiniumyl)-porphyrin (*n*=2, 3, 4) and its selective binding to native and synthetic DNAs, Biophys. J. 83 (2002) 371–381.
[11] Y.A. Lee, S. Lee, T.S. Cho, S.W. Han, S.K. Kim, Binding mode of *meso*-tetrakis(*N*-metylpyridinium-4-yl)porphyrin to poly[d(I-C)$_2$]: effect of amino group at the minor groove of poly[d(G-C)$_2$] on the porphyrin–DNA interaction, J. Phys. Chem., B 106 (2002) 11351–11355.
[12] T. Uno, K. Hamasaki, M. Taniguchi, S. Shimabayashi, Binding of *meso*-tetrakis(*N*-methylpyridinium-4-yl)porphyrin to double helical RNA and DNA · RNA hybrids, Inorg. Chem. 36 (1997) 1676–1683.
[13] J. Ren, J.B. Chaires, Sequence and structural selectivity of nucleic acid binding ligands, Biochemistry 38 (1999) 16067–16075.
[14] Y.A. Lee, J. Kim, T. Cho, R. Song, S.K. Kim, Binding of *meso*-tetrakis(*N*-methylpyridium-4-yl)porphyrin to triplex oligonucleotides: evidence for the porphyrin stacking in the major groove, J. Am. Chem. Soc. 125 (2003) 8106–8107.
[15] N.V. Anantha, M. Azam, R.D. Sheardy, Porphyrin binds to quadruplexed T_4G_4, Biochemistry 37 (1998) 2709–2714.
[16] I. Haq, J.O. Trent, B.Z. Chowdhry, T.C. Jenkins, Interactive G-tetraplex stabilization of telomeric DNA by a cationic porphyrin, J. Am. Chem. Soc. 121 (1999) 1768–1779.
[17] O.L. Fedoroff, A. Rangan, V.V. Chemeris, L.H. Hurley, Cationic porphyrin promote the formation of i-motif DNA and bind peripherally by a nonintercalative mechanism, Biochemistry 39 (2000) 15083–15090.
[18] H. Han, D.R. Langley, A. Rangan, L.H. Hurley, Selective interaction of cationic porphyrin with G-quadruplex structures, J. Am. Chem. Soc. 123 (2001) 8902–8913.
[19] D. Shi, R.T. Wheelhouse, D. Sun, L.H. Hurley, Quadruplexs-interactive agents as telomerase inhibitors: synthesis of porphyrin and structure–activity relationship for the inhibition of telomerase, J. Med. Chem. 44 (2001) 4509–4523.
[20] R.F. Pasternack, E.J. Gibbs, J.J. Villafranca, Interaction of porphyrins with nucleic acids, Biochemistry 22 (1983) 2406–2414.
[21] L.G. Marzilli, D.L. Banville, G. Zon, Pronounced ^{1}H and ^{31}P NMR spectral changes on *meso*-tetrakis(*N*-methylpyridinium-4-yl)porphyrin binding to teradecaoligo-deoxyribonucleotides: Evidence for symmetric, selective binding to 5′CG3′ sequences, J. Am. Chem. Soc. 108 (1986) 4188–4192.
[22] R.F. Pasternack, The influence of ionic strength on the binding of a water soluble porphyrin to nucleic acids, Nucleic Acids Res. 14 (1986) 5919–5931.
[23] I.E. Borissevitch, S.C.M. Gandini, Photophysical studies of excited-state characteristics of *meso*-tetrakis(4-*N*-methyl-pyridiniumyl)porphyrin bound to DNA, J. Photochem. Photobiol., B Biol. 43 (1998) 112–122.
[24] S. Lee, S.H. Jeon, B.J. Kim, S.W. Han, H.G. Jang, S.K. Kim, Classification of CD and absorption spectra in the Soret band of H_2TMPyP bound to various synthetic polynucleotides, Biophys. Chemist. 92 (2001) 35–45.
[25] M. Sriram, G.A. van der Marel, H.L.P.F. Roelen, J.H. van Boom, A.H.J. Wang, , Structural consequences of a carcinogenic alkylation lesion on DNA: effect of O6-ethylguanine [e6G] on the molecular structure of d(CGC[e6G]AATTCGCG)–netropsin complex, Biochemistry 31 (1992) 11823–11834.
[26] P.M. Takahara, A.C. Rozenweig, C.A. Frederick, S.T. Lippard, Crystal structure of double-stranded DNA containing the major adduct of the anticancer drug cisplatin, Nature 377 (1995) 649–652.
[27] H.C. Becker, B. Nordén, DNA binding mode and sequence specificity of piperazinylcarbonyloxyethyl derivatives of anthracene and pyrene, J. Am. Chem. Soc. 121 (1999) 11947–11952.
[28] H.C. Becker, B. Nordén, DNA Binding thermodynamics and sequence specificity of chiral piperazinecarbonyloxyalkyl derivatives of anthracene and pyrene, J. Am. Chem. Soc. 122 (2000) 8344–8349.
[29] U. Ellervik, C.C.C. Wang, P.B. Dervan, Hydroxybenzamide/pyrrole pair distinguishes T · A from A · T base pairs in the minor groove of DNA, J. Am. Chem. Soc. 122 (2000) 9354–9360.
[30] J. Lah, G. Vesnaver, Binding of distamycin A and netropsin to the 12mer DNA duplexes containing mixed AT · GC sequences with at most five or three successive AT base pairs, Biochemistry 39 (2000) 9317–9326.
[31] S.H. Cho, K.H. Chin, F.M. Chen, Looped out and perpendicular: Deformation of Watson–Crick base pair associated with actinomycin D binding, Proc. Natl. Acad. Sci. 99 (2002) 6625–6630.
[32] M. Pitto, V. Saudek, V. Sklenar, Gradient-tailored excitation for single-quantum NMR spectroscopy of aqueous solutions, J. Biomol. NMR 2 (1992) 661–666.
[33] V. Sklenar, M. Pitto, R. Leppik, V. Saudek, Gradient-tailed water suppression for ^{1}H–^{15}N HSQC experiments optimized to retain full sensitivity, J. Magn. Reson., Ser. A 102 (1993) 241–245.
[34] D.J. States, R.A. Haeberkorn, D.J. Ruben, A two-dimensional nuclear Overhauser experiment with pure absorption phase in four quadrants, J. Magn. Reson. 72 (1982) 286–292.